Low Roll-Off and High Efficiency Orange Organic Light Emitting Diodes with Controlled Co-Doping of Green and Red Phosphorescent Dopants in an Exciplex Forming Co-Host

*Sunghun Lee, Kwon-Hyeon Kim, Daniel Limbach, Young-Seo Park, and Jang-Joo Kim**

An exciplex forming co-host is introduced in order to fabricate orange organic light-emitting diodes (OLEDs) with high efficiency, low driving voltage and an extremely low efficiency roll-off, by the co-doping of green and red emitting phosphorescence dyes in the host. The orange OLEDs achieves a low turn-on voltage of 2.4 V, which is equivalent to the triplet energy gap of the phosphorescent-green emitting dopant, and a very high external quantum efficiency (EQE) of 25.0%. Moreover, the OLEDs show low efficiency roll-off with an EQE of over 21% at 10 000 cdm^{-2}. The device displays a very good orange color (CIE of (0.501, 0.478) at 1000 cdm^{-2}) with very little color shift with increasing luminance. The transient electroluminescence of the OLEDs indicate that both energy transfer and direct charge trapping takes place in the devices.

1. Introduction

Orange emitting organic light emitting diodes (OLEDs) are important in order to achieve highly efficient hybrid tandem white OLEDs, in which a blue fluorescent (FL) and an orange phosphorescent emitting system are connected by using a charge generation unit.[1] These hybrid tandem white OLEDs take advantage of a stable blue fluorescent unit with a long device lifetime and a high efficiency orange phosphorescent unit, and are the most widely used structure for displays and solid state lighting. There are two possible ways to construct an orange phosphorescent OLED. One way is to utilize a single orange emitting phosphorescent material. The other way is to utilize both green and red emitting phosphorescent materials. The first method has the advantages of easy fabrication and color stability with increasing luminance over the second method. Various heavy metal complexes which emit an orange color have been reported, based on platinum, iridium, and osmium as the heavy metal.[2,3] However, it is difficult to synthesize an orange emitting phosphorescent dye covering both the green and red regions of the spectrum, resulting in a low color rendering index (CRI) and a low color gamut (CG) when combined with a blue emission in white OLEDs. For instance, a very high efficiency orange OLED with an EQE of 27.5% showed a CRI value of 64 when combined with blue.[3] Solid state lighting and display applications require that the CRI and CG be over 80 and 80% of the NTSC standard, respectively.

The combination of green and red emissions leads to an orange emission with a broad spectrum. In other words, a co-doped green and red dopant in a single emitting layer can be considered as an orange emitter with a broad emission spectrum covering from green to red. Moreover emitting color can be tuned from green to red by adjusting their doping ratio. This quasi orange emitter results in white OLEDs with high CRI values compared to white OLEDs with just one type of orange emitting molecule when combined with a blue emitting layer. Large numbers of tandem white OLEDs incorporating orange OLEDs have been reported where green and red phosphorescent dyes are doped in a single emission layer (EML). Unfortunately, however, there are only a limited number of papers on the orange OLEDs themselves and their EQE values were less than 17.6% to our best knowledge.[4–6] Most of the works dealing with orange OLEDs are focused on assembled white OLEDs, and the orange OLEDs were not themselves studied in detail. Moreover, compared to the importance of orange OLEDs for white OLEDs, the efficiencies are significantly lower than the green and red OLEDs where the EQEs reach about 30%.[7,8]

S. Lee, K.-H. Kim, Prof. J.-J. Kim
WCU Hybrid Materials Program
Department of Materials Science and Engineering and the Center for Organic Light Emitting Diode
Seoul National University
Seoul, 151-744, Korea
E-mail: jjkim@snu.ac.kr

Dr. Y.-S. Park, Prof. J.-J. Kim
Department of Materials Science and Engineering and the Center for Organic Light Emitting Diode
Seoul National University
Seoul, 151-744, Korea

D. Limbach
Faculty 09: Chemistry
University Mainz
Mainz, 55128, Germany

S. Lee
Display Research Institute
Samsung Display Co., LTD., Giheung-Gu
Yongin-City, 446-711, Korea

DOI: 10.1002/adfm.201300187

Another problem of the phosphorescent orange OLEDs is from the large efficiency roll-off compared to fluorescent blue OLEDs, leading to a color change with increasing luminance. In order to achieve a stable color with increasing luminance in the tandem white OLEDs, orange OLEDs with a low efficiency roll-off are needed. However, low roll-off and high efficiency orange phosphorescent OLEDs have rarely been reported. An exciplex forming co-host can be considered as an advanced quasi-host material possessing its singlet and triplet excited state energy close to the energy difference between the LUMO of the acceptor (electron transporting material, ETM) and the highest occupied molecular orbital (HOMO) of the donor (hole transporting material, HTM) of the co-host materials. In our previous work we proposed exciplex forming co-hosts as a system to achieve a high EQE, low driving voltage and low efficiency roll-off at the same time.[8] This exciplex forming host system must play more importing role in orange emitting OLEDs doped with green and red dopants because of its broad emission zone to get color stability with increasing current density.

In this work, we report highly efficient orange OLEDs where green and red phosphorescent dopants are doped in an exciplex forming co-host as the EML, realizing a high EQE, low driving voltage and low efficiency roll-off at the same time. The best orange OLED showed a maximum EQE of 25.0%, and an EQE of 24.3% at 1000 cdm^{-2} and 21.2% at 10 000 cdm^{-2}, respectively. The CIE coordinates of the OLED were only slightly varied from (0.501, 0.488) at 1000 cdm^{-2} to (0.486, 0.491) at 10 000 cdm^{-2}. To the best of our knowledge, the EQE value of our present OLEDs is at least 1.5 times higher than that previously reported for orange OLEDs co-doped with green and red phosphorescent dyes. Furthermore, the operating voltage of 2.4 V is close to the triplet energy gap of the phosphorescent-green emitting dopant, and the efficiency roll-off is very low and close to that of a blue fluorescent device. In addition, the emission mechanism was investigated to understand the high efficiency and the low roll-off and high color stability with increasing current density.

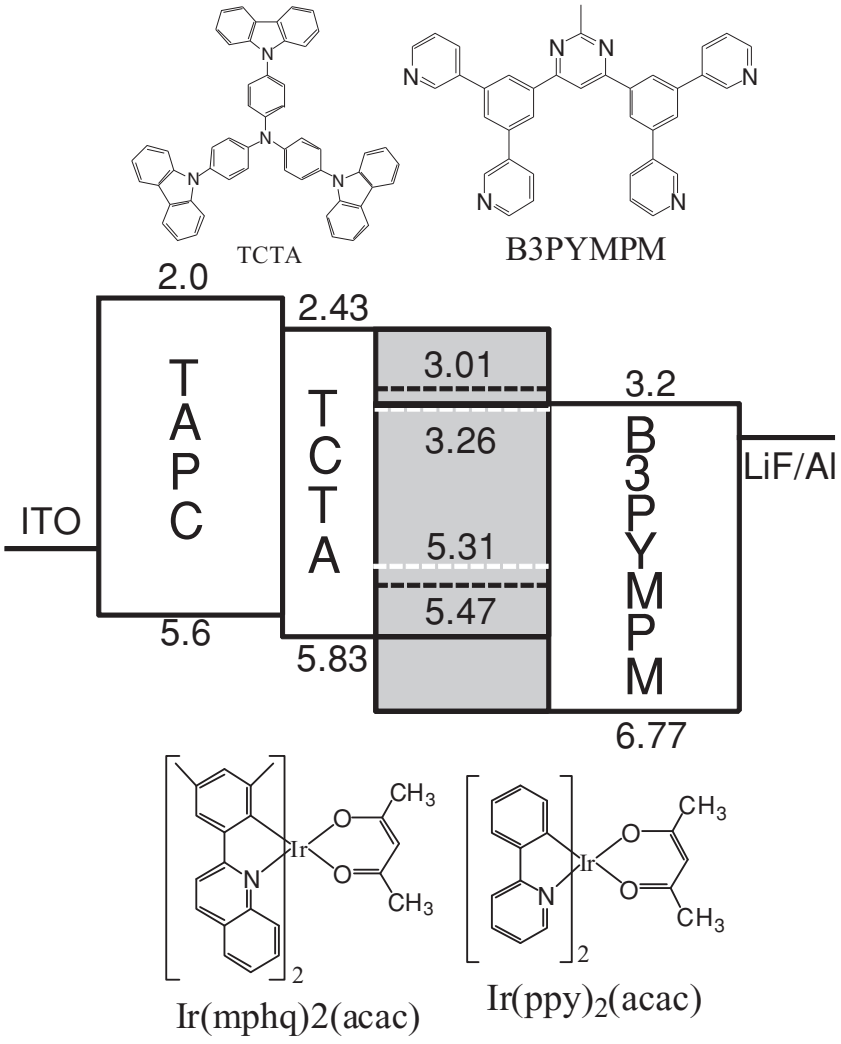

Figure 1. The molecular structures of TCTA, B3PYMPM, Ir(ppy)$_2$(acac), and Ir(mphq)$_2$(acac), and the device structure and energy level diagram of the OLEDs.

2. Results and Discussion

Figure 1 shows the schematic diagram of the device structure and the molecular structures used in the device. The device has a simple structure consisting of one hole injection material, one HTM and one ETM. Ir(ppy)$_2$(acac) [iridium(III) bis(2-phenylquinoline) acetylacetonate] and Ir(mphq)$_2$(acac) [iridium(III) (bis(2-(3,5-dimethylphenyl) quinoline acetylacetonate)] were used as the green and the red dopant, respectively. 4,4′,4″-tris(N-carbazolyl)-triphenylamine (TCTA) and bis-4,6-(3,5-di-3-pyridylphenyl)-2-methylpyrimi-dine (B3PYMPM) were chosen as the HTM and the ETM, respectively and used as the exciplex forming co-host for the EML because this co-host shows a higher triplet exciplex energy (2.5 eV) than those of the green (Ir(ppy)$_2$(acac), T_1 = 2.4 eV) and red (Ir(mphq)$_2$(acac), T_1 = 2.0 eV) phosphorescent dopants.[8] The device structure is as follows: indium tin oxide (ITO) (150 nm)/ TAPC (20 nm)/ TCTA (10 nm)/ TCTA:B3PYMPM: Ir(ppy)$_2$(acac):Ir(mphq)$_2$(acac) (30 nm, 8 wt%, × wt%)/ B3PYMPM (45 nm)/ LiF (0.7 nm)/ Al (100 nm), where TAPC is 1,1-bis-(4-bis(4-methyl-phenyl)-amino-phenyl)-cyclohexane. The molar ratio of TCTA to B3PYMPM in the EML was 1:1. The doping concentration of the green dopant was 8 wt% and the doping concentration of the red dopant was varied from 0.3 to 2 wt% to produce a combination of both colors, resulting in a perceived orange emission.

The absorption spectra of Ir(ppy)$_2$(acac) and Ir(mphq)$_2$(acac) are displayed in **Figure 2**a, with the emission spectra of the TCTA-B3PYMPM exciplex and Ir(ppy)$_2$(acac).

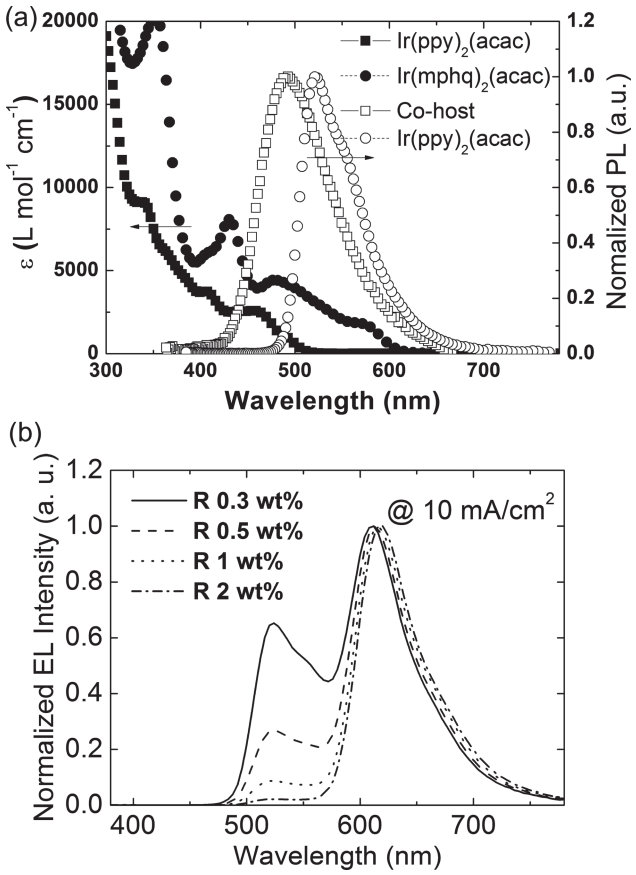

Figure 2. a) The normalized PL spectrum of the TCTA:B3PYMPM co-deposited film and $Ir(ppy)_2(acac)$, and the extinction coefficient of the $Ir(ppy)_2(acac)$, and $Ir(mphq)_2(acac)$. b) Normalized electroluminescence spectra of the OLEDs at a current density of 10mAcm^{-2}.

The overlaps between the PL spectra of the TCTA-B3PYMPM exciplex and $Ir(ppy)_2(acac)$ and the absorption spectrum of $Ir(mphq)_2(acac)$ are large enough to allow the energy transfer (ET) from the TCTA-B3PYMPM exciplex and $Ir(ppy)_2(acac)$ to $Ir(mphq)_2(acac)$. The Förster radii for the ET from the exciplex to $Ir(ppy)_2(acac)$ and $Ir(mphq)_2(acac)$ and from $Ir(ppy)_2(acac)$ to $Ir(mphq)_2(acac)$, calculated from the data, are 5.6, 7.1, and 8.4 nm, respectively.[9] The normalized electroluminescent spectra of the OLEDs with different red doping concentrations at a current density of 10 mA cm^{-2} are shown in Figure 2b. The green peak of the OLEDs was significantly reduced as the $Ir(mphq)_2(acac)$ doping concentration increased, and the green emission completely disappeared if the concentration of the red dopant was larger than 2 wt%. A very good orange color with the CIE coordinate of (0.491, 0.487) was obtained at 10 mA cm^{-2} when the concentration of the red dopant was 0.3 wt%. By using this orange OLED with blue emitter connected by using a charge generation unit, the CRI value of the tandem white OLED can reach 87.6, which is good enough for high quality lighting.

Figure 3a shows the current density–voltage–luminance (*J–V–L*) characteristics of the OLEDs. The driving voltage of the OLEDs was slightly reduced as the red doping concentration increased. The driving voltages at 10 mAcm^{-2} were 4.4, 4.3, 4.1, and 4.1 V for the OLEDs with red dopant concentrations of 0.3, 0.5, 1, and 2 wt%, respectively. The reduced driving voltage with increasing the doping concentration of the red dopant indicates that there is direct trapping of charges at the red dopant sites, as well as charge transport through the dopants when the doping concentration is higher than 1 wt% in the OLEDs. The turn-on voltage of the OLEDs was 2.4 V, which is the same as the triplet energy gap (2.4 eV) of the phosphorescent emitting dopant, $Ir(ppy)_2(acac)$. In addition, the driving voltage of the OLEDs at 5 mAcm^{-2} and 30 mAcm^{-2} were ≈3.7–3.9 V and ≈4.9–5.3 V, respectively. These low over-potentials can be achieved by the exciplex forming co-host system.[8]

Figure 3b shows the EQE and the power efficiency of the OLEDs, and the details of the performances of the OLEDs are summarized in **Table 1**. The 0.3 and 0.5 wt% OLEDs showed high EQEs and low efficiency roll-offs. However, the 1 and 2 wt% devices showed significantly lower EQEs than the 0.3 and 0.5 wt% OLEDs. The direct trapping of charges in the red dopant combined with its low PL quantum yield might have the effect of reducing the EQE. In contrast, the low doping concentrations of 0.3 and 0.5 wt% of the red dopant do not significantly perturb the charge transport and the resulting balance in the EML. This was confirmed by the facts that the *J–V* characteristics and the EQEs of the orange OLEDs with the doping concentrations of 0.3 and 0.5 wt% of the red dopant are comparable with that of a similarly structured green OLED.[8] The best orange OLED, doped with 0.3 wt% of $Ir(mphq)_2(acac)$, showed a maximum EQE of 25.0% and a peak power efficiency of 60.3 lm W^{-1}. To the best of our knowledge, the EQE of our present OLED is almost 1.5 times higher than that of previously reported values for green and red co-doped orange OLEDs. Moreover, the roll off of the efficiency is extremely low with an EQEs of 24.3% at 1000 cdm^{-2} and 21.2% at 10 000 cdm^{-2}.

Spectral shifts of the devices with increasing current density were investigated by plotting the radiance spectra normalized by their corresponding current density (radiance/current density). **Figure 4**a–d show the normalized EL spectra of the OLEDs with $Ir(mphq)_2(acac)$ concentrations of 0.3, 0.5, 1, and 2 wt% at the current densities of 1, 5, 10, and 30 mAcm^{-2}, respectively. The insets in Figure 4a–d show the color changes in the CIE 1931 chromaticity coordinates. All the devices showed small shifts in the color coordinates, even though the devices with higher red doping concentrations showed better color stability with increasing current density. The CIE coordinates of the OLED with the doping concentration of 0.3 wt% of the red dopant changed from (0.501, 0.488) at 1000 cdm^{-2} to (0.486, 0.491) at 10 000 cdm^{-2}. It is interesting to note that the green peaks in the EL spectra of the OLED retained an almost constant as the current density increased. Only the red peaks in the EL spectra of the OLEDs were reduced as the current density increased.

The variation in the efficiencies and spectral changes with the doping concentration of the red dopant and with the current density must be related to the emission mechanism of the green and red light in the OLEDs. The emission mechanism was investigated using the transient electroluminescence (EL) at red (616 nm) and green (524 nm) wavelengths of the orange OLEDs, which are shown in **Figure 5**a for different red doping

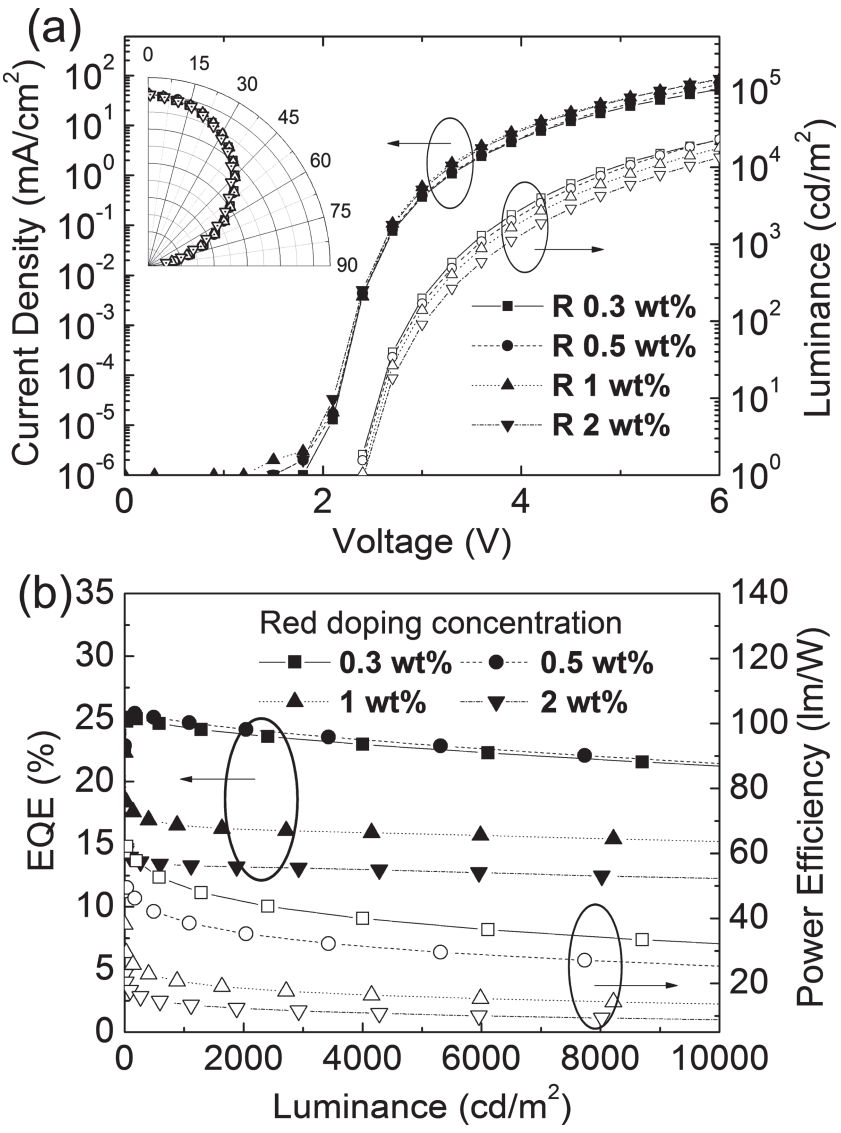

Figure 3. a) The current density–voltage–luminance characteristics of the OLEDs. Inset shows the angular distribution of the calculated number of photons from the measured EL spectra. b) The corrected EQE and the power efficiency of the OLEDs.

concentrations. The turn–on region in the normalized transient EL shows a faster turn–on of the green emission than that of the red emission in all the OLEDs, indicating that an energy transfer from the green to the red dopant takes place. In the turn–off region, transient overshoots are observed after the voltage pulse was turned off, and the height of the overshoot increases as the red doping concentration increases. The overshoot appears earlier with an increasing reverse turn–off voltage and later with a positive turn–off voltage, as shown in Figure 5b. These overshoots in the transient EL curves can be interpreted as being due to charge carrier accumulation or trapping in the red dopant.[10,11] The extensive charge trapping may have a negative effect in terms of the efficiency by exciton-polaron quenching, electric field induced quenching, and so on. This is also observed in our devices, where the efficiency is reduced with increasing concentration of the red dopant. The delayed saturation times of the transient EL for the red and green emission with increasing red doping concentration can be explained by the reduced hole mobility in the EML coming from the charge trapping effect due to the red dopant. It is interesting to note that the green emission also shows a transient overshoot after the turn-off of the pulse, in contrast to the green OLED without the red dopant, where no overshoot was observed.[8] This indicates that the charge trapping in the red dopant induces the overshoot, even in the green emission. Combination of the delayed turn-on of the red emission and the existence of the overshoot in the turn-off region indicate that both energy transfer from the green dopant to the red dopant and the direct charge trapping in the red dopant take place in the devices.

More information on the emission mechanisms can be obtained from the spectral shifts shown in Figure 4. All the spectra were deconvoluted into red and green portions and then the EQEs of the red peak were calculated. The roll-off characteristics of the red portions of the EQE in the EL spectra of the OLEDs are shown in **Figure 6**. The green emissions in the OLEDs were almost constant with increasing current density as shown in Figure 4. The lower doping concentration of the

Table 1. The details of the performances of the OLEDs.

Ir(mphq)$_2$(acac) concentration	Voltage [V]/ Luminance [cd/m^2]			CIE (x, y)		EQE (%)			Power efficiency [lm/W]		
	Turn-on	@10 mA/cm^2	@30 mA/cm^2	@10 mA/cm^2	@30 mA/cm^2	Max.	@10 mA/cm^2	@30 mA/cm^2	Max.	@1000 cd/m^2	@5,000 cd/m^2
Green OLED[8] (ITO 150 nm)	2.4/3.6	4.2/5244	5.1/16030	(0.339, 0.619)	(0.339, 0.617)	25.7	23.6	20.7	107.8	86.2	65.7
0.3 wt%	2.4/1.9	4.4/4005	5.3/11730	(0.491, 0.487)	(0.482, 0.494)	25.0	22.6	20.2	62.1	49.9	38.3
0.5 wt%	2.4/1.6	4.3/3425	5.2/10700	(0.562, 0.425)	(0.553, 0.433)	25.4	23.3	21.0	49.5	39.1	30.0
1 wt%	2.4/1.1	4.1/1634	4.9/5982	(0.619, 0.375)	(0.613, 0.380)	22.3	16.1	15.6	38.1	20.4	15.9
2 wt%	2.4/0.9	4.1/1117	4.9/4278	(0.65, 0.348)	(0.647, 0.351)	14.5	13.2	12.9	22.7	13.6	10.4

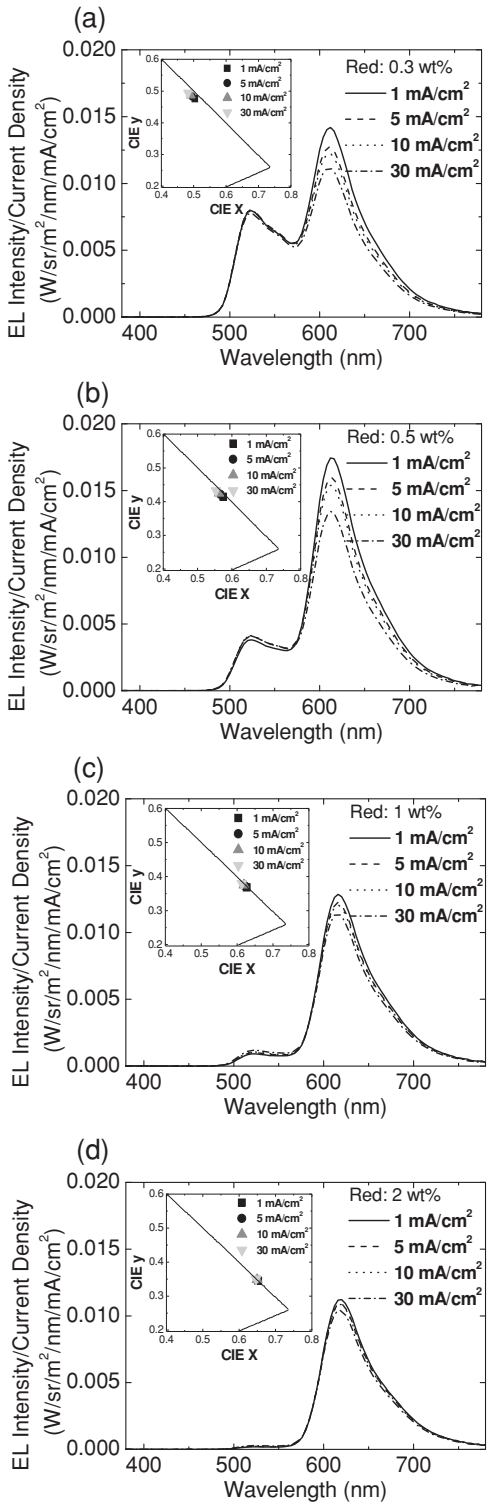

Figure 4. The EL spectra normalized by the current density of the OLED, at various current densities of 1, 5, 10, and 30 $mAcm^{-2}$: a) 0.3 wt% $Ir(mphq)_2(acac)$, b) 0.5 wt% $Ir(mphq)_2(acac)$, c) 1 wt% $Ir(mphq)_2(acac)$, and d) 2 wt% $Ir(mphq)_2(acac)$. Inset shows the CIE chromaticity coordinates of the OLEDs at the various current densities of 1, 5, 10, and 30 $mAcm^{-2}$.

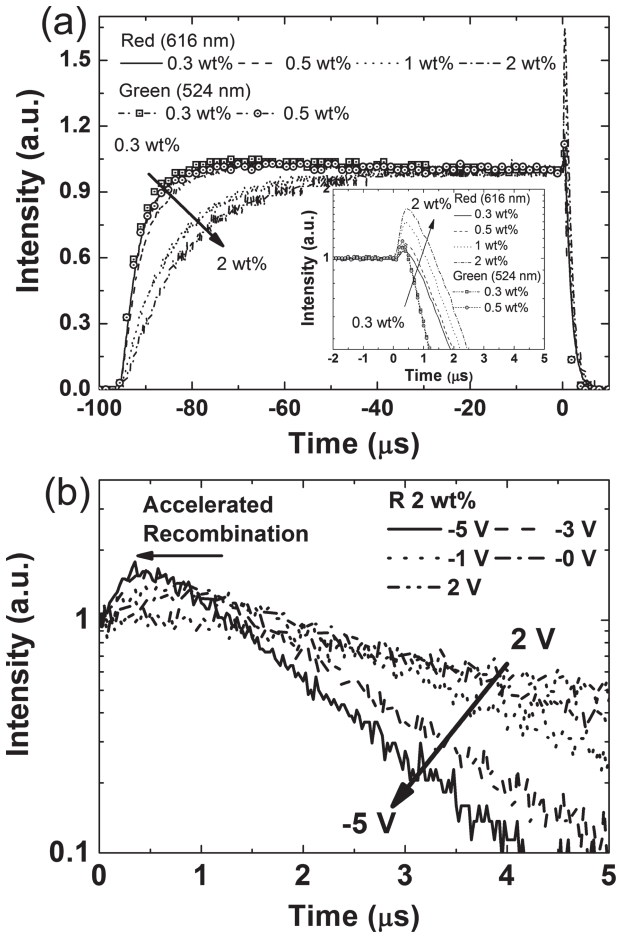

Figure 5. a) The normalized time resolved electroluminescent characteristics of the OLEDs. Inset shows the magnified transient electroluminescence around the turn-off region. b) Transient EL signals of the OLED with an $Ir(mphq)_2(acac)$ concentration of 2 wt% after the voltage pulse is turned off and different voltages are applied in the off-state (from –5 to 2 V).

red dopant resulted in a fast reduction of the EQE in the red emission as the current density increased. The roll-off characteristics can be explained by the bleaching of the red dopant with increasing current density, especially when the dopant concentration is low. In other words, the probability for the red dopant to exist in the excited (ground) state increases (decreases) with increasing current, so that direct charge trapping and energy transfer from the host and the green dopant at high current are limited. The behavior of the fast roll-off in the red portion of the EQE with decreasing red doping concentration at various current densities is an evidence of this concentration bleaching mechanism. Another plausible origin is the triplet-polaron quenching by the accumulated charges in the red dopant. It is difficult at this stage to identify which mechanism is dominant in the OLEDs and further study is required to clarify this.

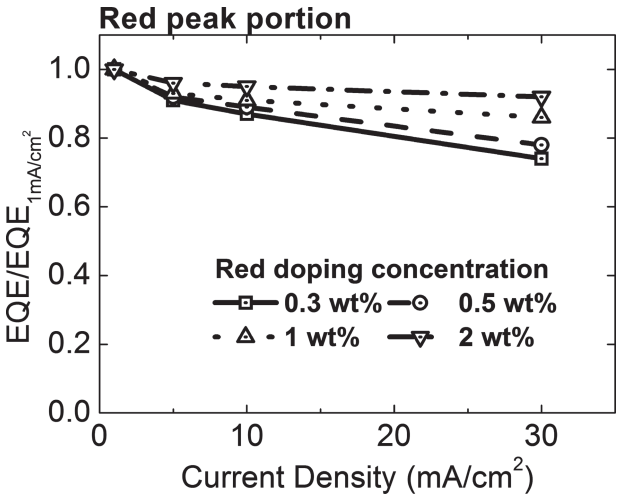

Figure 6. The EQE of the red peak portion normalized by the EQE of the red peak portion of the OLEDs at 1 mAcm^{-2} vs current density.

3. Conclusions

In summary, we successfully developed high performance orange OLEDs by co-doping green and red dopants in an exciplex-forming co-host. The OLEDs with the red doping concentration of 0.3 wt% showed well balanced orange emissions and achieved a low turn-on voltage of 2.4 V, which is equivalent to the triplet energy gap of the phosphorescent green emitting dopant, and a very high maximum EQE of 25.0%. In addition, the OLED showed a low efficiency roll-off with an EQE of 21% at 10 000 cdm^{-2}. This orange OLED has a large potential to produce high efficiency white OLEDs with a high CRI, low driving voltage, low efficiency roll-off and minimal color shift with increasing luminance.

4. Experimental Section

The OLEDs were fabricated by thermal evaporation onto cleaned glass substrates precoated with 150-nm-thick ITO. Prior to the organic layer deposition, the ITO substrates were exposed to a UV-ozone flux for 10 min, following degreasing in acetone and isopropylalcohol. OLEDs with the following structure, ITO (150 nm)/TAPC (20 nm)/TCTA (10 nm)/TCTA:B3PYMPM:Ir(ppy)$_2$(acac):Ir(mphq)$_2$(acac) (30 nm, 8 wt%, × wt%)/B3PYMPM (45 nm)/LiF (0.7 nm)/Al (100 nm), were fabricated by thermal deposition at a base pressure of $<5 \times 10^{-7}$ Torr without breaking the vacuum. The molar ratio of TCTA to B3PYMPM in the EML was 1:1, the concentration of the green dopant was fixed at 8 wt%, and the doping concentration of the red dopant was varied with the values 0.3, 0.5, 1, and 2 wt%. All the organic layers were deposited at a rate of 1 Å/s except for the co-deposited emission layer, whose deposition rate was 2 Å/s in total, and the rates of LiF and Al were 0.1 and 4 Å/s, respectively. The HOMO and the LUMO (lowest unoccupied molecular orbital) levels of the organic materials were obtained from the published literature, except for Ir(mphq)$_2$(acac).[8] The HOMO level of the Ir(mphq)$_2$(acac) was obtained from cyclic voltammetry measurement, the LUMO level was calculated from the HOMO level and the optical energy gap obtained from the edge of the absorption spectrum. The current density, the luminance, and the EL spectra were measured using a Keithley 2400 programmable source meter and a SpectraScan PR650 (Photo Research). The angular distribution of the EL intensity was measured using a Keithley 2400 programmable source meter, a rotation stage and an Ocean Optics S2000 fiber optic spectrometer. The EQE and power efficiency of the OLEDs were calculated from the current density, the luminance, the EL spectra, and the angular distribution of the EL intensity data. The time resolved EL measurements were obtained by applying voltage pulses to the device corresponding to 30 mA cm^{-2} for the red and green emissions with a 100 μs width using an 8114A pulse generator (Agilent), and detecting the emission using an ACTON spectrometer (SpectraPro-300i) connected with a photomultiplier tube (Acton Research, PD-438). The detection wavelengths were 524 and 616 nm for the green and red emissions, which corresponded to the peak wavelengths of the Ir(ppy)$_2$(acac) and Ir(mphq)$_2$(acac) emissions, respectively. All signals were detected and integrated 1000 times by a 54642A oscilloscope (Agilent). The voltage applied to the OLEDs was measured over a 1 MΩ resistance parallel to the OLED.

Acknowledgements

This work was supported by the Industrial Strategic Technology Development Program (10035225, Development of core technology for high performance AMOLED on plastic) funded by MKE/KEIT.

Received: January 17, 2013
Published online: April 8, 2013

[1] a) T. K. Hatwar, J. P. Spindler, M. Kondakova, D. Giesen, J. Deaton, J. R. Vargas, *Proc. SID'10* **2010**, 778; b) S. Lee, J.-H. Lee, J.-H. Lee, J.-J. Kim, *Adv. Funct. Mater.* **2012**, *22*, 855; c) S. Lee, J.-H. Lee, K. H. Kim, S.-J. Yoo, T. G. Kim, J. W. Kim, J.-J. Kim, *Org. Electron.* **2012**, *13*, 2346

[2] a) Y. M. Cheng, G. H. Lee, P. T. Chou, L. S. Chen, Y. Chi, C. H. Yang, Y. H. Song, S. Y. Chang, P. I. Shih, C. F. Shu, *Adv. Funct. Mater.* **2008**, *18*, 183; b) M. Li, W.-H. Chen, M.-T. Lin, M. A. Omary, N. D. Shepherd, *Org. Electron.* **2009**, *10*, 863; c) M. Li, M.-T. Lin, W.-H. Chen, R. McDougald, R. Arvapally, M. Omary, N. D. Shepherd, *Phys. Status Solidi A* **2012**, *209*, 221; d) K. H. Lee, H. J. Kang, S. J. Lee, J. H. Seo, Y. K. Kim, S. S. Yoon, *Synth. Met.* **2011**, *161*, 1113; e) B. S. Du, C. H. Lin, Y. Chi, J. Y. Hung, M. W. Chung, T. Y. Lin, G. H. Lee, K. T. Wong, P. T. Chou, W. Y. Hung, H. C. Chiu, *Inorg. Chem.* **2010**, *49*, 8713; f) D.-S. Leem, S. O. Jung, S.-O. Kim, J.-W. Park, J. W. Kim, Y.-S. Park, Y.-H. Kim, S.-K. Kwon, J.-J. Kim, *J. Mater. Chem.* **2009**, *19*, 8824.

[3] R. Wang, D. Liu, H. Ren, T. Zhang, H. Yin, G. Liu, J. Li, *Adv. Mater.* **2011**, *23*, 2823.

[4] K. S. Yook, S. O. Jeon, C. W. Joo, J. Y. Lee, M. S. Kim, H. S. Choi, S. J. Lee, C.-W. Han, Y. H. Tak, *Org. Electron.* **2009**, *10*, 681.

[5] G. Schwartz, S. Reineke, T. C. Rosenow, K. Walzer, K. Leo, *Adv. Funct. Mater.* **2009**, *19*, 1319.

[6] F. S. Steinbacher, R. Krause, A. Hunze, A. Winnacker, *Org. Electron.* **2011**, *12*, 911.

[7] a) D. Tanaka, H. Sasabe, Y.-J. Li, S.-J.Su, T. Takeda, J. Kido, *Jpn. J. Appl. Phys.* **2007**, *46*, L10-L12; b) M. G. Helander, Z. B. Wang, J. Qiu, M. T. Greiner, D. P. Puzzo, Z. W. Liu and Z. H. Lu, *Science* **2011**, *332*, 944-947.

[8] Y.-S. Park, S. Lee, K.-H. Kim, S.-Y. Kim, J.-H. Lee, J.-J. Kim, *Adv. Funct. Mater.,* 2013,10.100/adfm.201300547.

[9] T. Förster, *Discuss. Faraday Soc.* **1959**, *27*, 7.

[10] C. Weichsel, L. Burtone, S. Reineke, S. Hintschich, M. Gather, K. Leo, B. Lüssem, *Phys. Rev. B* **2012**, *86*, 074204.

[11] R. Liu, Z. Gan, R. Shinar, J. Shinar, *Phys. Rev. B* **2011**, *83*, 245302.